# The delayed island mass effect: How islands can remotely trigger blooms in the oligotrophic ocean

Monique Messié, Anne Petrenko, Andrea M. Doglioli, Clement Aldebert, Elodie Martinez, Guillaume Koenig, Sophie Bonnet, Thierry Moutin

# The delayed island mass effect: How islands can remotely trigger blooms in the oligotrophic ocean

M. Messié[1,2,*], A. Petrenko[1], A.M. Doglioli[1], C. Aldebert[1],
E. Martinez[3], G. Koenig[1], S. Bonnet[1], and T. Moutin[1]

[1]Aix Marseille Université, Université de Toulon, CNRS, IRD, Mediterranean Institute of Oceanography (MIO), Unité Mixte 110, 13288 Marseille, France,
[2]Monterey Bay Aquarium Research Institute, Moss Landing, CA 95039, USA,
[3]University of Brest, Ifremer, CNRS, IRD, Laboratoire d'Océanographie Physique et Spatiale (LOPS), IUEM, 29200 Brest, France,
[*]corresponding author, monique@mbari.org

**Key points:**

- Previously undescribed delayed island mass effects can generate intense blooms decoupled from island fertilization both in time and in space
- These occur when diazotrophs slowly utilize excess phosphate and iron after a classical island effect while being advected away from islands
- The fertilizing impact of islands on phytoplankton may thus currently be largely underestimated in the oligotrophic ocean

## Abstract

In oligotrophic gyres of the tropical ocean, islands can enhance phytoplankton biomass and create hotspots of productivity and biodiversity. This "Island Mass Effect" (IME) is typically identified by increased chlorophyll concentrations next to an island. Here we use a simple plankton model in a Lagrangian framework to represent an unexplained open ocean bloom, demonstrating how islands could have triggered it remotely. This new type of IME, termed "delayed IME", occurs when nitrate is limiting, N:P ratios are low, and excess phosphate and iron remain in water masses after an initial bloom associated with a "classical" IME. Nitrogen fixers then slowly utilize leftover phosphate and iron while water masses get advected away, resulting in a bloom decoupled in time (several weeks) and space (hundreds of km) from island-driven nutrient supply. This study suggests that the fertilizing effect of islands on phytoplankton may have been largely underestimated.



## Plain language summary

In the poor and nutrient-depleted waters of the tropical Pacific, islands act as sources of nutrients fertilizing nearby waters. These nutrients are consumed by microscopic photosynthesizing algae, the phytoplankton. The resulting phytoplankton enrichments (blooms) in turn support productive ecosystems. This phenomenon, termed the "island mass effect", has been known for sixty years and is classically defined by increased chlorophyll (representing phytoplankton biomass) next to an island. Blooms also occur in the open ocean and are usually attributed to vertical processes such as mixing or uplifting that locally supply nutrients from subsurface reservoirs. In this paper, we demonstrate that a different type of island mass effect exists, where the phytoplankton response is delayed because they grow very slowly. These blooms are supported by the nitrogen fixer *Trichodesmium*. Since phytoplankton get carried away from islands by oceanic currents while they grow, this can lead to a bloom located hundreds of km away with no apparent connection to the islands. Nutrient inputs by islands followed by advection can thus trigger remote blooms in the open ocean. Our study suggests that the fertilizing effect of islands may currently be largely underestimated, particularly in the warm waters of the tropical Pacific where *Trichodesmimum* is common.



**Index terms**

4855 Phytoplankton
4815 Ecosystems, structure, dynamics, and modeling (0439)
4845 Nutrients and nutrient cycling (0470, 1050)
4512 Currents
4562 Topographic/bathymetric interactions

**Keywords:** island mass effect, nitrogen fixation, Lagrangian analysis, phytoplankton bloom, oligotrophic ocean, nutrient supply

# 1. Introduction

In the mostly oligotrophic tropical ocean, phytoplankton blooms sometimes do occur, dramatically increasing local production (Behrenfeld & Boss, 2014; Messié et al., 2006; Ryan et al., 2002; Wilson & Qiu, 2008; Wilson et al., 2008). These blooms are triggered by an unusual supply of nutrients often resulting from short-lived vertical transport (Johnson et al., 2010; Wilson & Qiu, 2008) driven by (sub)mesoscale oceanic circulation (Mahadevan, 2016; Ryan et al., 2002), winds (Menkes et al., 2016) or a combination of both (McGillicuddy et al., 2007). Additional processes initiating and enhancing blooms include vertically migrating phytoplankton (Wilson et al., 2008), dispersion/dilution (Lehahn et al., 2017), seasonal mixing followed by stratification (Dore et al., 2008; Moutin et al., 2018), and island-driven nutrient supply (Gove et al., 2016; Wilson & Qiu, 2008).

The fertilizing effect of islands on oceanic productivity has been known for decades. Termed the Island Mass Effect (IME) by Doty and Oguri (1956), this process is almost ubiquitous across the tropical Pacific (Gove et al., 2016). In its classical sense, the IME is characterized by an inverse relationship between distance to an island and phytoplankton biomass and/or productivity, often represented by surface chlorophyll concentration (Chl). Biological enrichments are not always confined near the islands; Chl can peak downstream when lee eddies form (Hasegawa et al., 2009; Messié et al., 2006) and Chl enrichments can be spread by currents over hundreds of km (Shiozaki et al., 2014; Signorini et al., 1999). However, including in these cases, IMEs described in the literature (hereafter "classical IMEs") always remain characterized by increased Chl spatially connected to an island.

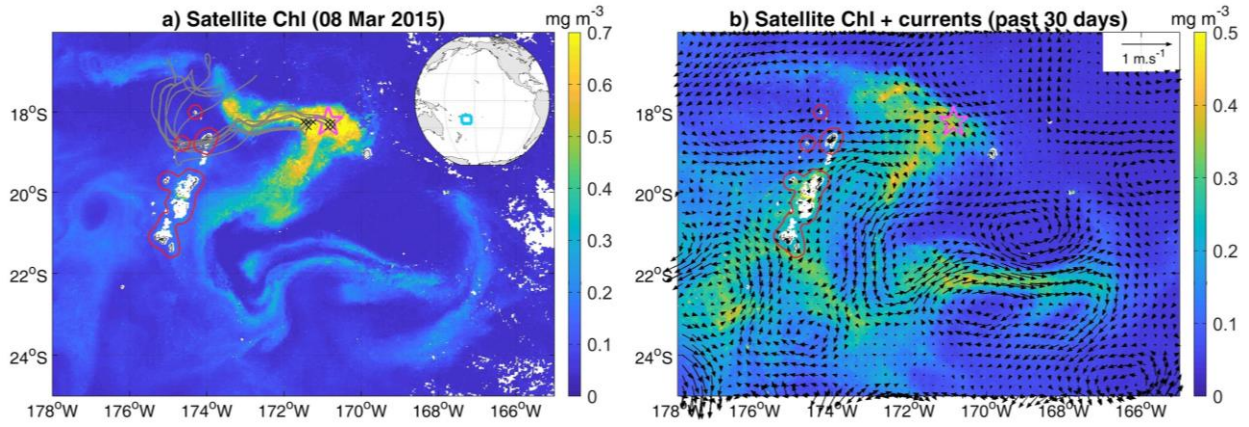


***Figure 1****: Satellite-derived contextual information. The Tonga islands are visible near 175°W; the region within 15 km of Tonga major coastlines is contoured in red. The pink star represents station LD-B occupied during March 15-20, 2015. a) Chl observed at the peak of the LD-B bloom. Reproducing previous results (de Verneil et al., 2017; Rousselet et al., 2018), grey lines display 60-day backward Lagrangian trajectories initialized at high-Chl patches near LD-B (Chl > 0.75 mg m$^{-3}$, black crosses). b) Chl and surface currents observed during the previous 30 days, providing information on water mass pathway and bloom generation (note the different colorbar).*

In this context, a spectacular bloom observed from space in the western tropical South Pacific early 2015 is puzzling (Fig. 1). The bloom occurred during the Oligotrophy to UlTra-oligotrophy PACific Experiment (OUTPACE) oceanographic cruise (Moutin et al., 2017), and was targeted by a Long Duration station (LD-B) due to its unusually high Chl for the region (> 0.9 mg m$^{-3}$). In order to study fine-scale physical-biological coupling, high resolution measurements were

performed when the vessel reached the bloom a week after its satellite-detected peak. Surprisingly, physical data revealed a stratified water column with no evidence of mixing, upwelling or submesoscale activity (de Verneil et al., 2017). At the same time, shipboard $^{15}N_2$ isotopic measurements unveiled very high nitrogen fixation rates sustaining nearly all new primary production (Caffin et al., 2018a), mostly supported by the diazotroph *Trichodesmium* (Bonnet et al., 2018). While nitrogen fixation is common in the region (Bonnet et al., 2017, 2018; Shiozaki et al., 2014), the process responsible for supplying enough nutrients to support this remarkably high biological production is unclear. High-phosphate waters had been advected from the eastern gyre (Bonnet et al., 2017), but the origin of iron remained a mystery, especially since diazotrophs need considerably more iron than non-diazotrophic phytoplankton (Berman-Frank et al., 2001). Local stratification ruled out vertical transport or mixing, and atmospheric deposition was low (Guieu et al., 2018). The only plausible hypothesis was offered by de Verneil et al. (2017), who suggested that iron was provided by an island contact. Indeed, although traveling on average westward, the eastern gyre waters passed near the Tonga islands early February, before they recirculated eastward toward LD-B (Fig. 1, grey).

In contrast to previous reports of island-driven *Trichodesmium* blooms (Shiozaki et al., 2014), however, the LD-B bloom is clearly disconnected from the Tonga islands (Fig. 1). The classical IME definition thus does not apply, and whether the bloom was triggered by islands remains to be demonstrated. We propose that the LD-B bloom is an undescribed type of IME, termed "delayed IME", where the phytoplankton respond so slowly to island fertilization that the bloom becomes separated from the islands as water masses are advected away. This hypothesis was tested first by investigating a potential nutrient release by the Tonga islands, and then by modeling the LD-B bloom using exclusively an island nutrient source and surface advection. Our simulations demonstrate how the Tonga islands could have indeed triggered the bloom, and provide a proof of concept for the existence of the delayed IME.

## 2. Materials and methods

### 2.1. Datasets and Lagrangian analysis

Satellite-derived surface Chl and currents were produced specifically for OUTPACE by Ssalto/Duacs and CLS with support from TOSCA/CNES. A complete description and validation can be found in de Verneil et al. (2017) and Rousselet et al. (2018). Briefly, surface Chl (available December 2$^{nd}$, 2014 to May 10$^{th}$, 2015, 1/50° daily) were obtained from Suomi/NPP/VIIRS measurements and computed as 5-day weighted averages; resulting concentrations agree well with *in situ* underway Chl (Rousselet et al., 2018). Surface currents (1/8° daily) combine absolute geostrophic velocities, wind-induced Ekman circulation relative to 15 m, and a cyclogeostrophy correction. These custom products provide higher spatial and temporal resolution, and better quality, than the typically available global products. Following Gove et al. (2016), shallow pixels were removed as they were potentially contaminated by bottom reflectance (white pixels near Tonga in Fig. 1: minimum depth < 30m according to ETOPO1 bathymetry, extended by one additional pixel in all directions). Precipitation was obtained from the Global Precipitation Measurement project (GPM IMERG v06, 0.1° daily, Huffman et al., 2019).

Ninety-day forward and backward Lagrangian trajectories, initialized at the center of each of the 83 current pixels located within 15 km of the major Tonga coastlines (15-km Tonga region, red contour in Fig. 1), were computed for each of the 160 days of the Chl time period. The Lagrangian diagnostic tool Ariane was used (Blanke & Raynaud, 1997), with a time step of 0.1 day. East/west water mass origin was defined for each pixel as the mean longitude during the previous 90 days minus the pixel longitude, as eastern waters are likely phosphate-rich (Bonnet et al., 2017; Moutin et al., 2008). Along-trajectory Chl was obtained by spatially interpolating smoothed Chl maps from the nearest day, generated to minimize data noise and gaps due to clouds using 2 iterations of spatial median filtering followed by a temporal linear interpolation of gaps not exceeding 5 days. For each trajectory, the average Chl 5-10 days upstream was termed Chl_upstream, and the Chl increase when passing by the islands was defined as $\Delta$Chl = Chl(0) - Chl_upstream (see Fig. S1).

## 2.2. The growth-advection approach

A simple plankton model was used, representing three nutrients (nitrogen N, phosphate P, and iron Fe), two phytoplankton (non-diazotrophic phytoplankton *Phy* and *Trichodesmium Tri*), and one zooplankton (*Z*) (Text S1, Fig. S2). Beyond its $N_2$-fixing capability, *Tri* differs from *Phy* by its much slower maximum growth rate (0.27 $d^{-1}$ vs. 1 $d^{-1}$) and its closure term (grazing for *Phy* vs. death for *Tri*, see details in Text S1). *Tri* death includes a programmed cell death (PCD), likely responsible for the LD-B bloom demise (Spungin et al., 2018), by which *Trichodesmium* blooms can collapse in a few days in response to nutrient stress (Berman-Frank et al., 2004). Modeled Chl follows assumed C:Chl ratios for *Phy* and *Tri*. The full model description, equations and parameters are given in Text S1 and Table S1.

The plankton model was coupled to island-driven nutrient supply and oceanic advection using a "growth-advection" method developed off California (Messié & Chavez, 2017). The method considers the evolution of plankton communities within the surface mixed layer of a water mass, as triggered by a fertilization process (here the IME) and advected by surface currents. Concretely, plankton biomass is simulated over time following an initial input of nutrients, and mapped on Lagrangian trajectories. Initial conditions constrain the intensity and timing of the Chl peaks and surface currents dictate their location.

Daily simulations were initialized within the 15-km Tonga region at the same locations as Lagrangian trajectories, with initial plankton concentrations constrained by Chl_upstream (Text S1). Initial nutrient concentrations N(0), P(0), and Fe(0) represent island-driven nutrient supply plus upstream concentrations (only for P). Because N-limited *Phy* grows faster and drives the initial bloom, N(0) was set proportional to $\Delta$Chl. P(0) was proportional to N(0) in Redfield proportions, with an additional P source when water masses originated from the east. Finally, the Tonga islands being volcanic, the island bedrock and/or sediments are likely iron-rich and can represent a significant source of iron (Palacios, 2002; Blain et al., 2008; Raapoto et al., 2019). Submarine groundwater discharge may also release iron, particularly for small tropical islands like Tonga (Moosdorf et al., 2015). Past studies found links between IMEs and surface currents with no evidence of upwelling, and proposed that turbulent mixing entrains iron-rich waters (Signorini et al., 1999; Martinez & Maamaatuaiahutapu, 2004). Fe(0) was thus proportional to current speed. All initialization parameters are given in Table S2.

Daily runs were computed from December 2$^{nd}$, 2014 to April 15$^{th}$, 2015 by mapping 90-day plankton model output initialized daily onto the corresponding forward Lagrangian trajectory.

Horizontal and vertical mixing was neglected (see Messié & Chavez (2017) for more details on the method). The daily runs were then combined into 1/8° daily gridded maps by keeping, for each day and each pixel, the maximum value from all runs. The maximum rather than the mean was used to avoid unrealistic dilution by low-Chl trajectories. A 5-day weighted average was then computed, following the method applied to satellite Chl.

### 2.3. Model optimization

The model solution depends on a number of constants, used to parameterize the plankton model and its initialization (Tables S1 and S2). Most of the plankton model parameters were obtained from the literature and/or from OUTPACE measurements. Some parameters were unknown either because of a process never having been modeled before, namely the PCD, or because no data was available to constrain them, such as parameters controlling initialization in the island vicinity (which was not sampled during OUTPACE). These parameters were first manually roughly tuned so that the model approximately represented satellite Chl. The corresponding model solution reproduced the major Chl blooms, although their timing was off by a few days (Fig. S3). Then, the parameters were fine-tuned using a gradient-based optimization method in order to best fit observations of satellite Chl (Text S2). The method optimized a cost function based on RMS differences of modeled and satellite Chl in delayed IME regions; classical IMEs were thus not optimized and were overestimated (Fig. S3). Details on the cost function, the optimization method and its results are provided in Text S2 and Fig. S3.

## 3. Results and discussion

### 3.1. Island-driven nutrient supply

A significant satellite Chl increase when passing by the islands (ΔChl) reveals an island-driven supply of nutrients supporting a classical IME. Two high-ΔChl events were observed during the period of study (Fig. 2a, blue shading), indicating that the Tonga islands can effectively act as a nutrient source. At the peak of both events (January 11$^{th}$ and February 9$^{th}$, 2015), ΔChl represented a > 90% increase relative to upstream Chl. The eastern origin of water masses during both events (Fig. 2b) indicates that waters were likely phosphate-rich but nitrate- and iron-depleted (Bonnet et al., 2017; Moutin et al., 2008). Islands must have thus supplied at least nitrate and/or iron to support the Chl increase.

Islands can supply nutrients through several processes, including wind-driven coastal upwelling, uplifting and mixing in lee eddies, land runoff, atoll lagoon flushing, coral reef benthic processes, and iron enrichment from the island platform (Gove et al., 2016; Hasegawa et al., 2009; Palacios 2002; Signorini et al., 1999). No correspondence was found between ΔChl and sea surface temperature, waves, or tides, so upwelling and lagoon flushing were unlikely. Island runoff was a possibility since both classical IMEs coincided with precipitation events (Fig. 2c). The Tonga islands considered here (part of the Vava'u and Ha'apai groups) are mostly low volcanic coral islands, but Vava'u slopes up to 200m-high cliffs in the north and rain could trigger significant runoff. However, not all precipitation events coincided with a Chl increase near the islands. Precipitation may thus be a necessary, but not sufficient, condition to trigger a classical IME. Surface currents and ΔChl are significantly correlated (r = 0.56 with a lag of 4-6

days, p<<0.01), and delayed bloom water mass origin coincides with strong currents (Fig. 2d diamonds), supporting the hypothesis of an additional iron source related to currents.

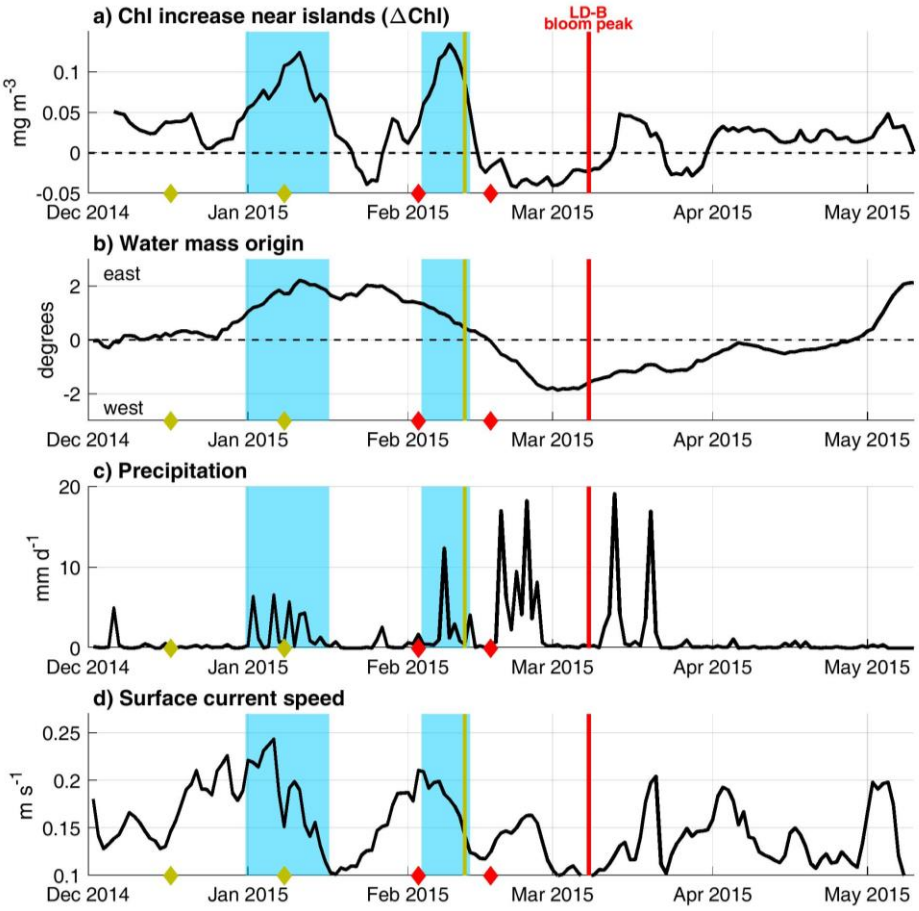


***Figure 2:*** *Characterization of the Tonga classical IME and its potential drivers. All variables were averaged over the 15-km Tonga region. Blue shading highlight times of significant Chl increase near islands, defined as ΔChl > 0.05 mg m$^{-3}$. The red line marks the LD-B bloom peak, and red diamonds circumscribe the period when 80% of its island-origin water masses* traveled through the 15-km Tonga region (*defined as along-trajectory satellite Chl > 0.7 mg m$^{-3}$ within 2 days of the bloom peak in the LD-B region, Fig. S3). Dark yellow similarly displays the delayed SW bloom peak and origin (see section 3.3).*

## 3.2. Biological evolution following island fertilization

The temporal evolution of satellite Chl downstream of Tonga along the Lagrangian trajectories (Fig. S1) clearly displays the classical IME in a significant number of trajectories, peaking within a few days. Interestingly, Chl usually displayed a second, separate peak weeks later. No significant water mass cooling was observed, so additional vertical nutrient inputs were unlikely. We propose that the two successive plankton blooms were supported by the same island-driven nutrient supply, indicating that two phytoplankton types responded to island fertilization with different time lags. *Trichodesmium* grow slower than most phytoplankton (Capone et al., 1997) and were thus likely responsible for the second bloom (delayed IME), as observed at LD-B (Bonnet et al., 2018). The first bloom (classical IME) was likely supported by non-diazotrophic phytoplankton, because another diazotroph species would have consumed all available phosphate and iron, preventing the delayed bloom from occurring.

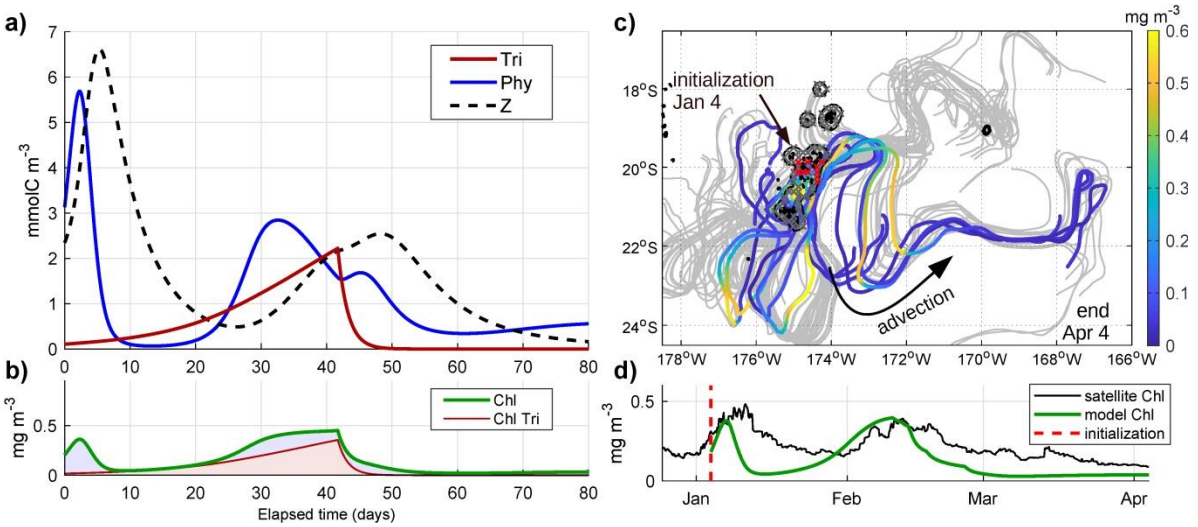


***Figure 3****: Example of plankton model output (left) and growth-advection run initialized on January 4$^{th}$, 2015 (right). a) Modeled plankton biomass as a function of time, following initialization corresponding to median conditions at the red crosses in c). b) Corresponding modeled Chl, total (green line) and of Tri (dark red line). Both the intensity and timing of the two Chl peaks depend on initial conditions. c) Ninety-day forward trajectories (grey or color) initialized at grey and red crosses near the Tonga islands. Along-trajectory modeled Chl is displayed in color for a few example trajectories initialized at the red crosses (between 19-20.5°S for ΔChl > 0.05 mg m$^{-3}$ and currents > 0.2 m s$^{-1}$). d) Time series of modeled (green) and observed (black) along-trajectory Chl, averaged for the example trajectories. The shape of the modeled delayed Chl peak is different in d than b, because its timing differs across the trajectories being averaged in d due to varying initial conditions. See Text S1 and S2 regarding underestimated Chl in non-bloom conditions.*

The plankton model was used to represent the temporal evolution of non-diazotrophic phytoplankton (*Phy*) and *Trichodesmium* (*Tri*) after an initial supply of nutrients (Fig. 3a,b). The model represents a classical IME paradigm where *Phy* blooms within a few days. Nitrate exhaustion and predation terminate this early bloom after about one week. The model additionally predicts a separate, *Tri*-dominated later peak: the delayed IME. It occurs because *Tri* grows slowly and utilizes leftover phosphate and iron over several weeks. A secondary *Phy* peak is also observed around the *Tri* maximum, supported by nutrients released by *Tri* that, in turn, re-enhance the bloom. Similar biological production enhancements due to *Trichodesmium* nutrient release have been observed previously (Bonnet et al., 2016; Caffin et al., 2018b). Once phosphate and/or iron stress become too high, the PCD causes the *Tri* bloom to collapse.

When considering advection by surface currents, the early and late Chl maxima translate into a peak near the islands (classical IME) and peaks in several locations away from the islands (delayed IME), respectively (Fig. 3c). Not all trajectories display both an early and late Chl peak, consistent with satellite observations (Fig. S1). This is because *Phy* and *Tri* are decoupled in the model, *Phy* being primarily a function of ΔChl (controlling N(0)) and *Tri* of currents and water mass origin (controlling Fe(0) and excess P relative to N, respectively). The modeled Chl peak timing is close to the timing of early and late peaks observed in satellite along-trajectory Chl (Fig. 3d). *Tri*'s slow growth rate is thus responsible for the temporal decoupling between island fertilization and delayed IME, while advection by surface currents explains their spatial decoupling.

### 3.3. Classical and delayed IME impacts on phytoplankton

Time-varying satellite Chl maps highlight several major blooms during the period of study (Fig. 4, see also Movie S1): east (E) bloom close to Tonga in January, southwest (SW) bloom downstream of Tonga in mid-February, and LD-B bloom early March. These are separate from near-island Chl increases depicted in Fig. 2 (blue shading). Island-driven Chl enrichments were examined by combining individual growth-advection daily runs (e.g., Fig. 3c) into gridded daily maps. The result is remarkably similar to satellite Chl (Fig. 3d, 4 and Fig. S3), requiring only island fertilization and oceanic advection to reproduce major bloom timing and spatial features. Using the *Tri-Phy* dominance as an indicator of delayed vs. classical IME, the model identifies the E bloom as a classical IME and the SW and LD-B blooms as delayed IMEs. These represent two different situations: the SW bloom remained connected to the islands as water masses recirculated towards Tonga, while the LD-B bloom became separated as water masses got advected away. Both were preceded by island-driven fertilization and a classical IME by about one month (Fig. 2a).

The model's success in representing satellite Chl has two implications. First, island-driven nutrient supply and oceanic advection are sufficient to reproduce the LD-B bloom, supporting the hypothesis that the bloom was a delayed IME fertilized by the Tonga islands. Second, the growth-advection model represents all satellite-detected blooms, indicating that they were likely triggered by island effects. This suggests that islands were not only responsible for the LD-B bloom, but even more remarkably were the primary driver of Chl variability in the region for the period of study. Island-driven iron inputs, in addition to submarine hydrothermal iron sources (Guieu et al., 2018), may thus contribute to explain the hotspot of nitrogen fixation found in the western tropical South Pacific (Bonnet et al., 2017). Indeed, top 30m iron concentrations along the OUTPACE transect were highest around the Tonga islands (0.98 ± 0.16 nM), an area where deeper concentrations were relatively low (0.59 ± 0.21 nM) (Guieu et al., 2018).

The prevalence of delayed IMEs is difficult to quantify beyond the region and period of study. A detailed Lagrangian analysis, as performed here, would be needed to determine if an open-ocean bloom was fueled by island effects or by local processes. Our analysis required daily high-resolution Chl and current satellite products, that were specifically produced for OUTPACE and are unfortunately not available on a regular basis. Nevertheless, an analysis of VIIRS chlorophyll near Tonga does suggest that delayed IMEs may be common in the region, particularly in summer (Fig. S4). More generally, delayed IMEs may occur when conditions support diazotrophy (warm temperatures and stratified waters) in the presence of islands supplying iron and/or phosphate. Regions such as Melanesia's eastern boundary (i.e., Fiji and Tonga islands) appear particularly favorable, as westbound phosphate-rich waters intersect volcanic, iron-rich islands.

Regardless of their frequency, delayed IMEs can be responsible for unusually strong phytoplankton blooms in a largely oligotrophic environment. At the peak of the two delayed IMEs described here, Chl reached values close to 1 mg $m^{-3}$, a tenfold increase relative to background concentrations. While classical IMEs can reach similar concentrations, the duration and spatial extent of delayed IMEs were much higher in the model (Fig. 3, 4). Summing the corresponding modeled Chl over space and time, delayed IMEs were responsible for enrichments (> 0.1 mg $m^{-3}$) over twice as high as those of classical IMEs, even though classical IMEs were overestimated (Fig. S3).

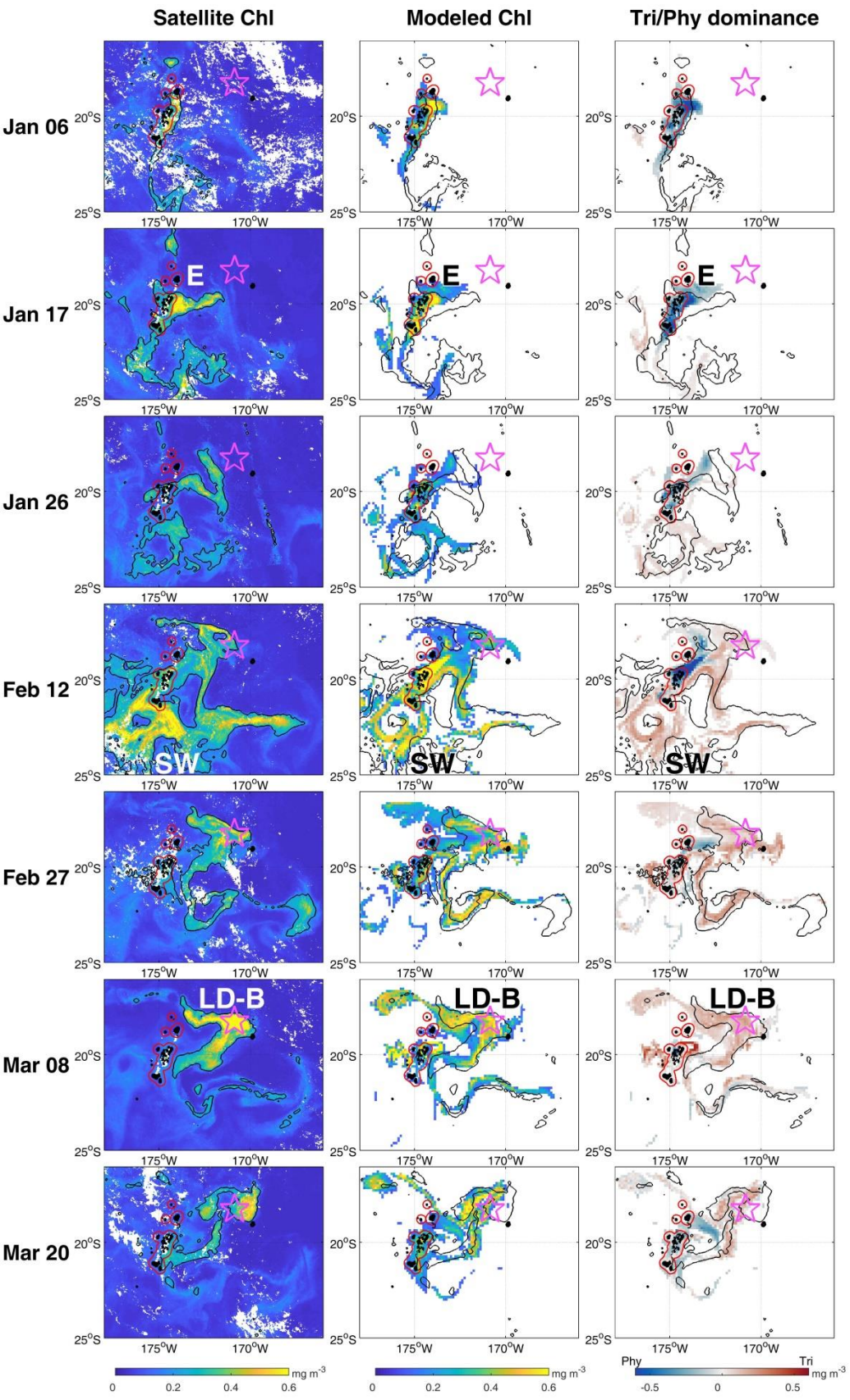
Satellite Chl
Modeled Chl
Tri/Phy dominance
Jan 06
Jan 17
Jan 26
Feb 12
Feb 27
Mar 08
Mar 20
E
SW
LD-B
20°S
25°S
175°W
170°W
mg m-3
0
0.2
0.4
0.6
Phy
Tri
-0.5
0
0.5

***Figure 4****: Chl temporal evolution as observed from satellite and modeled using the growth-advection method (see also Movie S1). Left: daily satellite Chl. Middle: model output, keeping only pixels where modeled Chl > 0.1 mg $m^{-3}$. Right: Tri-Phy dominance defined as Tri Chl minus Phy Chl, also representing the classical (Phy-dominated, blue) vs. delayed (Tri-dominated, red) IMEs. In all panels, black contours represent the 0.2 mg $m^{-3}$ Chl contour from the satellite smoothed product, red contours encircle the 15-km Tonga region, and the pink star is the LD-B location.*

## 4. Conclusion

This study provides strong evidence for the existence of delayed IMEs, a previously undescribed type of island effect where the bloom is spatially and temporally decoupled from island fertilization. Contrary to classical IMEs where phytoplankton respond quickly, resulting in a bloom near an island, delayed IMEs are supported by slow-growing nitrogen fixers such as *Trichodesmium*. They can occur when conditions are favorable for diazotrophy (e.g., warm stratified waters) and excess iron and phosphate remain in water masses after a classical IME.

Delayed IMEs represent situations where the time scale for biology (weeks) is much longer than the advection time scale (days), which is very unusual in the ocean and results in a temporal and spatial decoupling between nutrient supply processes and phytoplankton response. Such a mismatch between biological and physical time scales can lead to unexpected blooms in stratified waters with no apparent origin. In particular, delayed IMEs do not match the classical IME definition of Chl increase nearby islands and would not be identified by traditional IME detection methods such as a Chl contour (Shiozaki et al., 2014) or an inverse relationship between Chl and distance to an island (Gove et al., 2016). Without *in situ* subsurface data revealing the lack of vertical processes, these remote blooms could be mistakenly attributed to (sub)mesoscale activity. Island effects on phytoplankton biomass and productivity may thus have been largely underestimated.

## Acknowledgements and data

M.M. was funded by the European Union's Horizon 2020 research and innovation programme under the Marie Skłodowska-Curie grant agreement SAPPHIRE No. 746530. This research is a contribution of the OUTPACE project (http://doi.org/10.17600/15000900), funded by the Agence Nationale de la Recherche (ANR-14-CE01-0007-01), the LEFE-CyBER program (CNRS-INSU), the Institut de Recherche pour le Développement (IRD), the GOPS program (IRD) and TOSCA/CNES (BC T23, ZBC 4500048836). The growth-advection method was developed under NASA grant 80NSSC17K0574, and the optimization method under French ANR/DGA project Turbident (ANR16-ASTR-0019-01). We thank Louise Rousselet and Stéphanie Barrillon for their help with Ariane, Isabelle Pujol and Guillaume Taburet (CLS) for their support with satellite-derived products, and Eric Pape for useful comments and text edits. Satellite chlorophyll and currents are available at http://www.obs-vlfr.fr/proof/php/outpace/outpace_data.php, and precipitation at https://disc.gsfc.nasa.gov/datasets/GPM_3IMERGDF_V06/summary.

# References


Behrenfeld, M. J., & Boss, E. S. (2014), Resurrecting the ecological underpinnings of ocean plankton blooms, *Ann. Rev. Mar. Sci.*, 6, 167-194, https://doi.org/10.1146/annurev-marine-052913-021325

Berman-Frank, I., Cullen, J. T., Shaked, Y., Sherrell, R. M., & Falkowski, P. G. (2001), Iron availability, cellular iron quotas, and nitrogen fixation in Trichodesmium, *Limnol. Oceanogr.*, *46*(6), 1249-1260, https://doi.org/10.4319/lo.2001.46.6.1249

Berman-Frank, I., Bidle, K., Haramaty, L., & Falkowski, P. G. (2004), The demise of the marine cyanobacterium, Trichodesmium spp., via an autocatalyzed cell death pathway, *Limnol. Oceanogr.*, *49*, 997-1005, https://doi.org/10.4319/lo.2004.49.4.0997

Blain, S., Sarthou, G., & Laan, P. (2008), Distribution of dissolved iron during the natural iron-fertilization experiment KEOPS (Kerguelen Plateau, Southern Ocean), *Deep Sea Res. Part II*, *55*(5-7), 594-605, https://doi.org/10.1016/j.dsr2.2007.12.028

Blanke, B., & Raynaud, S. (1997), Kinematics of the Pacific Equatorial Undercurrent: an Eulerian and Lagrangian approach from GCM results, *J. Phys. Oceanogr.*, *27*(6), 1038-1053, https://doi.org/10.1175/1520-0485(1997)027<1038:KOTPEU>2.0.CO;2

Bonnet, S., Berthelot, H., Turk-Kubo, K., Cornet-Barthaux, V., Fawcett, S., Berman-Frank, I., et al. (2016), Diazotroph derived nitrogen supports diatom growth in the South West Pacific: A quantitative study using nanoSIMS, *Limnol. Oceanogr.*, *61*(5), 1549-1562, https://doi.org/10.1002/lno.10300

Bonnet, S., Caffin, M., Berthelot, H., Grosso, O., Benavides, M., Helias-Nunige, S., et al. (2018), In-depth characterization of diazotroph activity across the western tropical South Pacific hotspot of N2 fixation (OUTPACE cruise), *Biogeosciences*, *15*(13), 4215-4232, https://doi.org/10.5194/bg-15-4215-2018

Bonnet, S., Caffin, M., Berthelot, H., & Moutin, T. (2017), Hot spot of N2 fixation in the western tropical South Pacific pleads for a spatial decoupling between N2 fixation and denitrification, *Proc. Natl. Acad. Sci.*, *114*(14), E2800-E2801, https://doi.org/10.1073/pnas.1619514114

Caffin, M., Berthelot, H., Cornet-Barthaux, V., Barani, A., & S. Bonnet, S. (2018b), Transfer of diazotroph-derived nitrogen to the planktonic food web across gradients of N2 fixation activity and diversity in the western tropical South Pacific Ocean, *Biogeosciences*, *15*(12), 3795-3810, https://doi.org/10.5194/bg-15-3795-2018

Caffin, M., Moutin, T., Foster, R. A., Bouruet-Aubertot, P., Doglioli, A. M., Berthelot, H., et al. (2018a), N2 fixation as a dominant new N source in the western tropical South Pacific Ocean (OUTPACE cruise), *Biogeosciences*, *15*(8), 2565-2585, https://doi.org/10.5194/bg-15-2565-2018

Capone, D. G., Zehr, J. P., Paerl, H. W., Bergman, B., & Carpenter, E. J. (1997), Trichodesmium, a globally significant marine cyanobacterium, *Science*, *276*(5316), 1221-1229, https://doi.org/10.1126/science.276.5316.1221

Dore, J. E., Letelier, R. M., Church, M. J., Lukas, R., & Karl, D. M. (2008), Summer phytoplankton blooms in the oligotrophic North Pacific Subtropical Gyre: Historical perspective and recent observations, *Prog. Oceanogr.*, *76*(1), 2-38, https://doi.org/10.1016/j.pocean.2007.10.002

Doty, M. S., & Oguri, M. (1956), The island mass effect, *J. Cons. Int. Explor. Mer.*, *22*(1), 33-37, https://doi.org/10.1093/icesjms/22.1.33

Gove, J. M., McManus, M. A., Neuheimer, A. B., Polovina, J. J., Drazen, J. C., Smith, C. R., et al. (2016), Near-island biological hotspots in barren ocean basins, *Nat. Commun.*, *7*, 10581, https://doi.org/10.1038/ncomms10581

Guieu, C., Bonnet, S., Petrenko, A., Menkes, C., Chavagnac, V., Desboeufs, C., Maes, C., & Moutin, T. (2018), Iron from a submarine source impacts the productive layer of the Western Tropical South Pacific (WTSP), *Sci. Rep.*, *8*, https://doi.org/10.1038/s41598-018-27407-z

Hasegawa, D., Lewis, M. R., & Gangopadhyay, A. (2009), How islands cause phytoplankton to bloom in their wakes, *Geophys. Res. Lett.*, *36*, L20605, https://doi.org/10.1029/2009GL039743

Huffman, G. J., Stocker, E. F., Bolvin, D. T., Nelkin, E. J., & Tan, J. (2019), GPM IMERG Final Precipitation L3 1 day 0.1 degree x 0.1 degree V06, Edited by Andrey Savtchenko, Greenbelt, MD, Goddard Earth Sciences Data and Information Services Center (GES DISC), Accessed: 05/27/2019, doi:10.5067/GPM/IMERGDF/DAY/06

Johnson, K. S., Riser, S. C., & Karl, D. M. (2010), Nitrate supply from deep to near-surface waters of the North Pacific subtropical gyre, *Nature*, *465*, 1062-1065, https://doi.org/10.1038/nature09170

Lehahn, Y., Koren, I., Sharoni, S., d'Ovidio, F., Vardi, A., & Boss, E. (2017), Dispersion/dilution enhances phytoplankton blooms in low-nutrient waters, *Nat. Commun.*, *8*, 14868, https://doi.org/10.1038/ncomms14868

Mahadevan, A. (2016), The impact of submesoscale physics on primary productivity of plankton, *Ann. Rev. Mar. Sci.*, *8*(1), 161-184, https://doi.org/10.1146/annurev-marine-010814-015912

Martinez, E., & Maamaatuaiahutapu, K. (2004), Island mass effect in the Marquesas Islands: Time variation, *Geophys. Res. Lett.*, *31*(18), https://doi.org/10.1029/2004gl020682

McGillicuddy, D. J. J., Laurence, A. A., Bates, N. R., Bibby, T., Buesseler, K. O., Carlson, C. A., et al. (2007), Eddy/wind interactions stimulate extraordinary mid-ocean plankton blooms, *Science*, *316*(5827), 1021-1026, https://doi.org/10.1126/science.1136256

Menkes, C. E., Lengaigne, M., Lévy, M., Ethé, C., Bopp, L., Aumont, O., et al. (2016), Global impact of tropical cyclones on primary production, *Global Biogeochem. Cycles*, *30*(5), 767-786, https://doi.org/10.1002/2015gb005214

Messié, M., & Chavez, F. P. (2017), Nutrient supply, surface currents, and plankton dynamics predict zooplankton hotspots in coastal upwelling systems, *Geophys. Res. Lett.*, *44*(17), 8979-8986, https://doi.org/10.1002/2017GL074322

Messié, M., Radenac, M.-H., Lefèvre, J. & Marchesiello, P. (2006), Chlorophyll bloom in the western Pacific at the end of the 1997-98 El Niño: the role of the Kiribati Islands, *Geophys. Res. Lett.*, *33*, L14601, https://doi.org/10.1029/2006GL026033

Moosdorf, N., Stieglitz, T., Waska, H., Dürr, H. H., & Hartmann, J. (2015), Submarine groundwater discharge from tropical islands: a review, *Grundwasser*, 20(1), 53-67, https://doi.org/10.1007/s00767-014-0275-3

Moutin, T., Doglioli, A. M., de Verneil, A., & Bonnet, S. (2017), Preface: The Oligotrophy to the UlTra-oligotrophy PACific Experiment (OUTPACE cruise, 18 February to 3 April 2015), *Biogeosciences*, *14*(13), 3207-3220, https://doi.org/10.5194/bg-14-3207-2017

Moutin, T., Karl, D. M., Duhamel, S., Rimmelin, P., Raimbault, P., Van Mooy, B. A. S., & Claustre, H. (2008), Phosphate availability and the ultimate control of new nitrogen input by nitrogen fixation in the tropical Pacific Ocean, *Biogeosciences*, *5*(1), 95-109, https://doi.org/10.5194/bg-5-95-2008

Moutin, T., Wagener, T., Caffin, M., Fumenia, A., Gimenez, A., Baklouti, M., et al. (2018), Nutrient availability and the ultimate control of the biological carbon pump in the western tropical South Pacific Ocean, *Biogeosciences*, *15*(9), 2961-2989, https://doi.org/10.5194/bg-15-2961-2018

Palacios, D. M. (2002), Factors influencing the island-mass effect of the Galapagos archipelago, *Geophys. Res. Lett.*, *29*(23), 2134, https://doi.org/10.1029/2002GL016232

Raapoto, H., Martinez, E., Petrenko, A. A., Doglioli, A. M., Gorgues, T., Sauzède, R., et al. (2019), Role of iron in the remarkable Marquesas island mass effect, *J. Geophys. Res. Oceans*, in press, https://doi.org/10.1029/2019JC015275

Rousselet, L., de Verneil, A., Doglioli, A. M., Petrenko, A. A., Duhamel, S., Maes, C., & Blanke, B. (2018), Large- to submesoscale surface circulation and its implications on biogeochemical/biological horizontal distributions during the OUTPACE cruise (southwest Pacific), *Biogeosciences*, *15*(8), 2411-2431, https://doi.org/10.5194/bg-15-2411-2018

Ryan, P. R., Polito, P. S., Strutton, P. G., & Chavez, F. P. (2002), Unusual large-scale phytoplankton blooms in the equatorial Pacific, *Prog. Oceanogr.*, *55*(3-4), 263-285, https://doi.org/10.1016/S0079-6611(02)00137-4

Shiozaki, T., Kodama, T., & Furuya, K. (2014), Large-scale impact of the island mass effect through nitrogen fixation in the western South Pacific Ocean, *Geophys. Res. Lett.*, *41*(8), 2907-2913, https://doi.org/10.1002/2014GL059835

Signorini, S. C., McClain, C. R., & Dandonneau, Y. (1999), Mixing and phytoplankton bloom in the wake of the Marquesas Islands, *Geophys. Res. Lett.*, *26*(20), 3121-3124, https://doi.org/10.1029/1999GL010470

Spungin, D., Belkin, N., Foster, R. A., Stenegren, M., Caputo, A., Pujo-Pay, M., et al. (2018), Programmed cell death in diazotrophs and the fate of organic matter in the western tropical South Pacific Ocean during the OUTPACE cruise, *Biogeosciences*, *15*(12), 3893-3908, https://doi.org/10.5194/bg-15-3893-2018

de Verneil, A., Rousselet, L., Doglioli, A. M., Petrenko, A. A., & Moutin, T. (2017), The fate of a southwest Pacific bloom: gauging the impact of submesoscale vs. mesoscale circulation on biological gradients in the subtropics, *Biogeosciences*, *14*(14), 3471-3486, https://doi.org/10.5194/bg-14-3471-2017

Wilson, C., & Qiu, X. (2008), Global distribution of summer chlorophyll blooms in the oligotrophic gyres, *Prog. Oceanogr.*, *78*(2), 107-134, https://doi.org/10.1016/j.pocean.2008.05.002

Wilson, C., Villareal, T. A., Maximenko, N., Bograd, S. J., Montoya, J. P., & Schoenbaechler, C. A. (2008), Biological and physical forcings of late summer chlorophyll blooms at 30N in the oligotrophic Pacific, *J. Mar. Syst.*, *69*(3-4), 164-176, https://doi.org/10.1016/j.jmarsys.2005.09.018